Monthly Notices of the ROYAL ASTRONOMICAL SOCIETY

MNRAS **484,** 2499–2513 (2019) doi:10.1093/mnras/stz024

Photometric characterization of NEOs: 3 Amor and 3 Apollo★

Eduardo Rondón,[1]† Plicida Arcoverde,[1] Filipe Monteiro,[1] Hissa Medeiros,[1] Giuliat Navas,[2] Daniela Lazzaro,[1] Jorge M. Carvano[1] and Teresinha Rodrigues[1]

[1]*Observatório Nacional, Rua Gal. José Cristino 77, 20921-400 Rio de Janeiro, Brazil*
[2]*Centro de Investigaciones de Astronomía, Apartado Postal 264, 5101-A Mérida, Venezuela*

Accepted 2019 January 1. Received 2018 December 31; in original form 2018 November 3

ABSTRACT

We report the results based on a complete photometric characterization method for six near-Earth objects (NEOs), determining the rotational period, the taxonomic classification, the $V - R$ colour, the absolute magnitude and the slope parameter. The data were acquired at the Observatório Astronômico do Sertão de Itaparica, for (138846) 2000 VJ61, 2016 WJ1 and (36236) 1999 VV, of the Apollo group, and (489337) 2006 UM, 2005 TF and (326683) 2002 WP, of the Amor group. The performed analysis enabled us to classify three objects in the S-complex, one in the C-complex and one as a V-type. An estimate of the effective diameter is also given for four of them. Throughout our work is evident the importance of performing a complete photometric characterization in order to derive reliable physical parameters. in particular, we show that the rotational lightcurve amplitude is a very important parameter that needs to be considered when deriving photometric magnitudes of NEOs.

Key words: minor planet – asteroids: individual: Amor – asteroids: individual: Apollo.

1 INTRODUCTION

The near-Earth object (NEO) population is constituted of small bodies with orbits that are close to, or even cross, that of the Earth. This population is usually divided into four distinct groups depending on their orbital parameters: Atiras, Amors, Apollo and Atens. The first two have Earth-approaching orbits while the last two cross the orbit of the Earth. Due to their serious threat to the Earth it is very important to know their physical properties, especially those that are relevant to the precise determination of their orbit. One of these properties is the rotation period and the spin direction, since accurate modelling of a NEO's trajectory requires inclusion of the Yarkovsky/YORP effects that depend on these parameters. In addition, the study of the physical properties of a large sample of NEOs can help understand the origin and evolution of the population as a whole, and is fundamental for planning future space missions.

Photometric observations of NEOs can be used to derive the rotational lightcurve, the phase curve and the photometric spectrum, which in turn allow the determination of the rotation period, the spin-axis orientation, the shape, the size, the colours and the taxonomy type (Harris et al. 1989; Pravec, Šarounová & Wolf 1996; Pravec, Wolf & Šarounová 1998; Whiteley, Tholen & Hergenrother 2002; Kaasalainen et al. 2004; Warner, Harris & Pravec 2009; Mommert et al. 2016; Erasmus et al. 2017; Perna et al. 2017; Vaduvescu et al. 2017). It should be stressed that, despite the existence of several dedicated works, these properties have been partially determined only for less than 10 per cent of the more than 19 000 NEOs known. For example, about 1300 objects have a rotational period with good reliability, i.e. a quality code greater than 2- according to the lightcurve database LCDB[1] (Warner et al. 2009), and among these just nearly 200 NEOs have a taxonomic classification derived from spectra.

In order to contribute to the international efforts aiming to increase the knowledge on the NEO population, the IMPACTON project[2] was designed to set up a facility dedicated to the study of these objects. Since 2011 the Observatório Astronômico do Sertão de Itaparica (OASI, Itacuruba, Brazil) has been operating an extensive observational campaign to obtain data for the physical characterization of a large sample of NEOs. In this paper we present the results obtained for six NEOs and discuss the methodology used to establish a complete photometric characterization of these objects.

The present paper is organized as follows: in Section 2 we give a description of the different observational methodologies and data reduction procedures used, in Section 3 we present and discuss the

★ Observations obtained at the Observatório Astronômico do Sertão de Itaparica (OASI, Itacuruba) of the Observatório Nacional (ON-Brazil), and with complementary observations at the Observatorio Astronómico Nacional Llano del Hato operated by Centro de Investigaciones de Astronomía (CIDA- Venezuela).

† E-mail: erondon@on.br

[1]http://www.minorplanet.info/lightcurvedatabase.html
[2]http://www.on.br/impacton/

techniques applied to derive the relevant physical parameters from the obtained data, and in Section 4 are given the results for each object separately. Finally, in Section 5 we summarize our results and conclusions.

2 OBSERVATIONS AND DATA REDUCTION

The observations presented here were performed between 2016 October and 2017 February at the Observatório Astronômico do Sertão de Itaparica (code Y28, OASI-Nova Itacuruba), within the framework of the IMPACTON project and at the Observatorio Astronómico Nacional Llano del Hato (OANLH) operated by the Centro de Investigaciones de Astronomía (CIDA-Venezuela).[3] Both observatories are equipped with 1-m telescopes and 2048 x 2048 pixel CCDs but have different fields of view: 11.8′ x 11.8′ at OASI and 20′ x 20′ at ONLH. At OASI, observations were performed using the *R*-Cousins filter to derive light and phase curves, and the $g - r - i - z$ Sloan Digital Sky Survey (SDSS) filters to obtain photometric spectra. The observations at OANLH were all performed using the *R*-Cousins filter.

In order to obtain the relative magnitudes (for lightcurves) and the photometric magnitudes (for phase curves and spectra), different observational strategies and data reduction procedures were applied for each case. In the first case the telescope was set in sidereal tracking and the NEO observed over one or more nights for several hours. Whenever necessary, the telescope pointing was changed to follow the object. The data reduction was performed using the MaxIm DL package, following the standard procedure in which the science image is corrected for master-bias, master-dark and master-flat. Relative magnitudes were then obtained for each image, by performing the difference between the instrumental magnitude of the NEO and of a field star of similar brightness (usually more than one star is used, to guarantee that it is not variable).

In the case of the photometric magnitudes, the telescope was set to differential tracking mode, but different observational strategies were used to derive phase curves or spectra. In the first case, the NEO and a standard star were observed three or four times over the night in the *R*-Cousins filter. At each time, three or more images were obtained, and the resulting magnitudes were then averaged to reduce the random error. Moreover, the whole procedure was repeated on different nights over one or more months to map different solar phase angles of the NEO. In the second case, i.e. to obtain the photometric spectrum, images of the NEO and a standard star were obtained alternating the filter between *g*, *r*, *i*, *z* and repeating the sequence three or four times over the night. The data reduction in both cases was performed using the IRAF package correcting the science image for bias, dark and flat frames. The instrumental magnitudes for the NEO and the standard star were determined through aperture photometry, using the photometric growth curve (Howell 1989) to determine the optimum aperture. The standard stars were used to compute the zero-point and the extinction coefficient of the night, and the respective uncertainties.

3 DERIVING PHYSICAL PARAMETERS

The lightcurve of an object is how its brightness varies over time. In the case of asteroids, this variation is assumed to be mainly due to the rotation of an irregular and/or elongated object. The rotation period and amplitude can thus be obtained by fitting the lightcurve to a Fourier series (Harris et al. 1989), as given in equation (1), where α is the solar phase angle (angle between the lines connecting the asteroid to the Sun and the Earth), ϕ is the rotational phase angle, $V(\phi)$ is the computed reduced magnitude at a phase angle α and time t, A_l and B_l are the Fourier coefficients, P is the rotational period, and t_0 is the zero-point time of the observation:

$$V(\phi) = A_0 + \sum_{l=1}^{n} [A_l \sin(2\pi l\phi) + B_l \cos(2\pi l\phi)]\,; \qquad \phi = \left(\frac{t - t_0}{P}\right). \tag{1}$$

On the other hand, the solar phase curve is how the brightness of an asteroid varies with changing solar illumination with respect to the observer. It is well known (Seeliger 1887; Gehrels, Coffeen & Owings 1964; Thorpe 1978; Bowell & Lumme 1979) that this curve exhibits a steep increase at small phase angles, also known as 'opposition surge', and a linear behaviour at larger solar phase angles. This non-linear behaviour is attributed to two phenomena: shadow-hiding and coherent backscattering (Hapke 1990, 1993, 2002). In 1985, the IAU Commission 20 adopted a two-parameter magnitude system for asteroids (Bowell et al. 1989) based on the application of the Lumme–Bowell photometric model (Lumme & Bowell 1981) to asteroid phase curves. This system, called the $H - G$ model, is expressed by equation (2), where $H(\alpha)$ is the reduced magnitude of an object located at 1 au from the Sun and the Earth, H_0 is the absolute magnitude and G is the slope parameter. The absolute magnitude is defined as the brightness of an asteroid at 1 au from the Sun and Earth and at $\alpha = 0^0$ (Verbiscer & Veverka 1995). The slope parameter describes the shape of the phase curve and is related to the surface albedo. Values of $G \approx 0$ produce steep phase curves and are associated with low-albedo objects, while larger values ($G \approx 1$) produce flatter phase curves and tend to be associated with higher albedos:

$$H(\alpha) = H_0 - 2.5\log[(1 - G)\Phi_1(\alpha) + G\Phi_2(\alpha)]. \tag{2}$$

A new system, denominated $H - G1 - G2$ (Muinonen et al. 2010), was adopted by IAU in 2012 to improve the modelling of the phase curve for high- and low-albedo asteroids. The model is expressed by equation (3), which is fitted to the data using the linear least-squares method:

$$H(\alpha) = H_0 - 2.5\log[G_1\Phi_1(\alpha) + G_2\Phi_2(\alpha) + (1 - G_1 - G_2)\Phi_3(\alpha)], \tag{3}$$

where H_0, G_1 and G_2 are the parameters of the model, the functions Φ_1 and Φ_2 are related to the linear part of the phase curve while Φ_3 is associated with the opposition effect. These functions are given, for $\alpha < 30^\circ$, by equations (4)–(6):

$$\Phi_1(\alpha) = 1 - \frac{6\alpha}{\pi} \tag{4}$$

$$\Phi_2(\alpha) = 1 - \frac{9\alpha}{\pi} \tag{5}$$

$$\Phi_3(\alpha) = \exp\left(-4\pi \tan^{2/3}\left(\frac{\alpha}{2}\right)\right). \tag{6}$$

More recently Penttilä et al. (2016) showed that, in general, the above basis functions are given in terms of cubic spline functions $\xi(\alpha)$ (tabulated in their work). Since Muinonen et al.'s model (2010) fails when the number of observations is small or when the data are of low accuracy, this problem is solved using a constrained

[3] http://www.cida.gob.ve/webcida/

non-linear least-squares algorithm to fit the data to the model (Penttilä et al. 2016). This is the approach used in the present work, since for most of the NEOs in our sample the data are sparse and sometimes have large errors. It is also important to note that, since our magnitudes were obtained in the *R*-Cousins filter, the fit to the phase curve gives H_{0R}. The absolute magnitude H_0 is then derived using colour transformations.

Lastly, the photometric spectrum of an asteroid shows how the reflectance varies with the wavelength and is directly related to the surface composition of the object. The behaviour of the spectrum thus can be used to derive a taxonomic classification. To derive the spectrum of the observed NEOs, the first step was to transform the colour measures $(m_g - m_r)_A$, $(m_r - m_i)_A$ and $(m_r - m_z)_A$ in the SDSS system by flux normalizing to the *r* band and removing the solar colours $(m_g - m_r)_\odot$, $(m_r - m_i)_\odot$, $(m_r - m_z)_\odot$[4] (equation 7). This is the same procedure used by Carvano et al. (2010) to derive a taxonomic classification for the asteroids from the SLOAN-MOC4 catalogue, producing templates for the identified classes. We thus compared each of our spectra with these templates and derived the taxonomic classification of the NEO, using a chi-squared best fit:

$$f_x = \frac{\left(\frac{f_x}{f_r}\right)_A}{\left(\frac{f_x}{f_r}\right)_\odot} = 10^{-0.4C_{x-r}};$$
$$C_{x-r} = (m_x - m_r)_A - (m_x - m_r)_\odot. \quad (7)$$

The procedures given above to derive solar phase curves and photometric spectra are valid only for spherical or non-rotating objects. It is noteworthy that, due to the elongated shape of most asteroids, their reduced magnitude can vary considerably. To correct for such an effect, the photometric magnitudes need to be referred to a common rotational phase. This is done using equations (8)–(10), where $\mathcal{A}$ is the amplitude ratio of the rotational lightcurves, as given by Zappala et al. (1990), and ϕ_0 is the phase offset. In this way, for each data set, we get a nominal correction $\Delta V'(\phi)$ that is computed with respect to the rotational phase at the time instant of the observation with the smaller error in that particular set. The value of the correction on each point is then chosen as the one that minimizes the dispersion of the curve. It is important to note, however, that the adopted procedure is valid only if the lightcurve is obtained during the same night, or on consecutive nights, where the amplitude ratio $\mathcal{A} \approx 1$:

$$V'(\phi) = \mathcal{A}V(\phi + \phi_0) \quad (8)$$

$$H_c(\alpha) = H(\alpha) - \Delta V'(\phi) \quad (9)$$

$$f_{xc} = f_x 10^{\Delta V'(\phi)}. \quad (10)$$

Finally, the absolute magnitude in the *R*-Cousins filter (H_{0R}), along with the visual albedo (ρ_v), and the colour $V - R$, can be used to derive the effective diameter ($\bar{D}$) using equation (11) (Fowler & Chillemi 1992; Harris & Lagerros 2002). In our case the visual albedo is taken directly from the literature or inferred from mean values of the taxonomic class of the object as given by Mainzer et al. (2011), and the colour $V - R$ is computed using the transformation equation between SDSS magnitudes and *UBVRcIc* given by

[4]http://www.sdss.org/dr12/algorithms/ugrizvegasun/

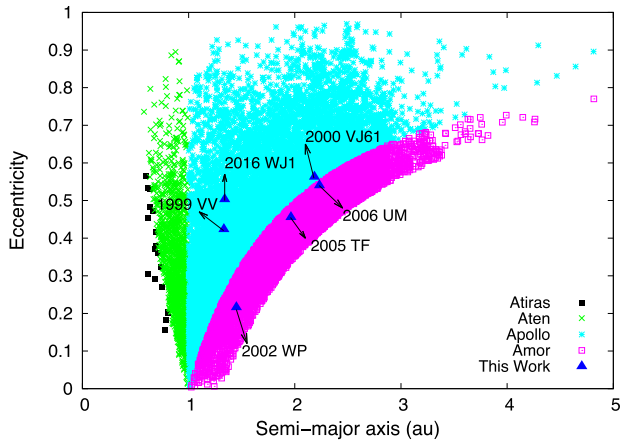

Figure 1. Distribution, in the semi-major versus eccentricity space, of all the known NEOs. The different symbols and colours indicate objects of the diverse groups: Atiras (black full squares), Aten (green crosses), Apollo (cyan stars), Amor (magenta squares), and objects studied in the present work (blue triangles).

Lupton (2005):

$$\bar{D} = \frac{1340 * 10^{-\frac{1}{5}(H_{0R}+V-R)}}{\sqrt{\rho_v}}. \quad (11)$$

4 RESULTS

We derived the photometric properties for six NEOs, i.e. three of the Amor group, (326683) 2002 WP, (489337) 2006 UM and 2005 TF, and three of the Apollo group, (36236) 1999VV, (138846) 2000 VJ61 and 2016 WJ1. The location of these objects in the semi-major axis versus eccentricity space is shown in Fig. 1 along with all the known NEOs.

In what follows we will present the results for each object separately, starting with those of the Amor group and followed by those of Apollo. It is important to note that all the objects were observed at OASI and just 2005 TF had complementary observations obtained at OANLH. In Appendix A the Fourier series coefficients A_l and B_l of the composite lightcurves are given for each asteroid, as well as the observational circumstances and the derived magnitudes for each set of data.

4.1 NEOs of the Amor group

4.1.1 (326683) 2002 WP

The period for this asteroid was calculated using data obtained on 2016 November 26, 28 and 29. The composite lightcurve was fitted with a sixth-order Fourier series. The derived period, $P = 6.261 \pm 0.002$ h, and the lightcurve amplitude, $A = 1.33$ mag (Fig. 2), are similar to that obtained by Vaduvescu et al. (2017) ($P = 6.273$ h) from observations on 2016 December 2, by Warner (2017b) ($P = 6.262$ h) from observations on 2016 November 23 and 25 and by Ditteon et al. (2018) ($P = 6.263$ h) from observations on 2016 November 28 to December 5.

The photometric spectrum for this asteroid was obtained from observations performed on 2016 November 26 and is shown in Fig. 3. In the figure we show the observed magnitudes, normalized at the *r* filter, indicated by black dots with corresponding error bars connected by the dotted line. These magnitudes are then corrected to account for the amplitude of the rotational lightcurve, and are shown

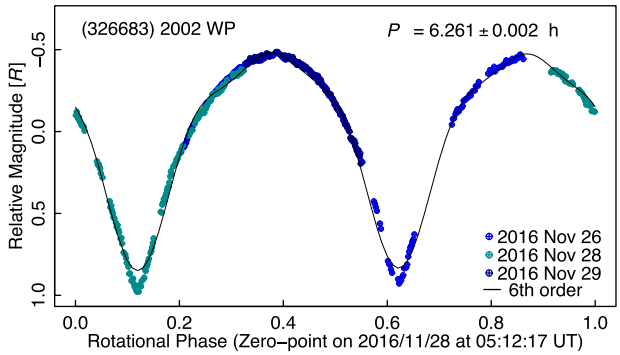

Figure 2. Composite lightcurve of the NEO (366683) 2002 WP along with the best Fourier fit (black line).

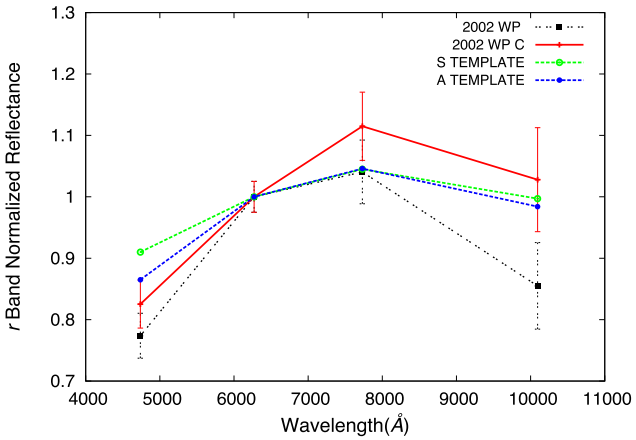

Figure 3. Photometric spectrum normalized to the r filter of the NEO (326683) 2002 WP. The points indicate the magnitude, and respective error, at the band centre for each filter. The diverse lines indicate the observed spectrum (black dotted line), the rotationally corrected spectrum (red solid line) and the templates of the S- (green dashed line) and A-type (blue dashed line) taxonomic classification from Carvano et al. (2010).

by the red dots connected by the solid red line. The significant difference among the two sets of magnitudes is due to the large amplitude of the rotational lightcurve as shown in Fig. 2. The chi-squared test, applied to several templates from the taxonomic scheme by Carvano et al. (2010), indicates that the A-type, of the S-complex, best fits the corrected spectrum. It is important here to note, however, that Carry et al. (2016) classify this asteroid as a D-type using data from the SLOAN-MOC4 catalogue. The discrepancy between the two classifications can be attributed to the large error in the z filter (of both spectra!) or the large rotational amplitude of this object, or is indicative of surface composition variations. More recently, Erasmus et al. (2017) also observed this NEO and classified it as S-type with a moderate probability (0.47) of belonging to this class. Although this classification is more in agreement with the spectrum given here, we believe that more data are needed to establish the real surface composition of this NEO.

Observations of this asteroid on 2016 November and December allowed magnitudes to be obtained at phase angles ranging from 6.9 to 22 degrees, represented by the black dots in Fig. 4. These observed magnitudes were then corrected to account for the rotational variations and are shown by the red squares in the figure. As expected, due to the large amplitude of the rotational lightcurve, the fit to the corrected magnitudes gives an error envelope much smaller

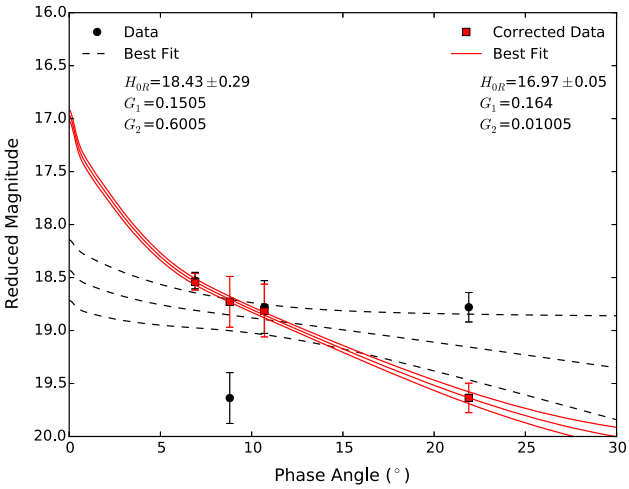

Figure 4. Phase curve of the asteroid (326683) 2002 WP. The black dotted curve and red solid curve represent the fits to the observed and rotationally corrected magnitudes, respectively. In both cases the central curve represents the best fit while the error envelope is given by the upper and lower curves.

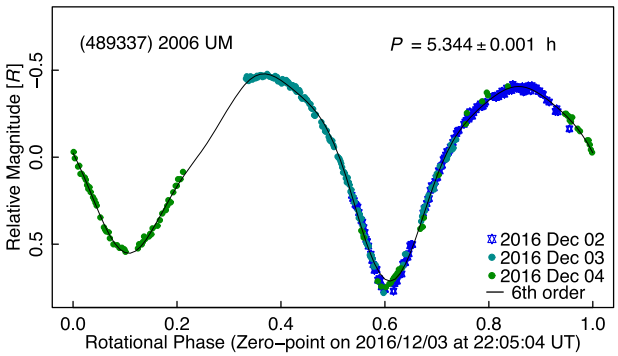

Figure 5. Composite lightcurve for the NEO (489337) 2006 UM, showing the best Fourier fit (black line).

than that to the observed ones. The derived absolute magnitude and slope parameters for this asteroid are: $H_{0R} = 16.97 \pm 0.05$, $G_1 = 0.164$ and $G_2 = 0.010\,05$. This asteroid is a good example of how important it is to take into account the rotational variations when deriving the absolute magnitude.

Finally, we computed an effective diameter of $\bar{D} = 0.771 \pm 0.19$ km using equation (11) with the above absolute magnitude and the colour $V - R = 0.486 \pm 0.035$, derived from our SLOAN colours, and a visual albedo of $\rho_v = 0.315 \pm 0.131$, given in Mainzer et al. (2016).

4.1.2 (489337) 2006 UM

This asteroid was observed from 2016 December 2–4, to derive its lightcurve. The data were fitted by a sixth-order Fourier series, giving a rotation period of $P = 5.344 \pm 0.001$ h and a composite lightcurve amplitude of $A = 1.191$ mag. The composite lightcurve is shown in Fig. 5 along with the best fit. A similar value, $P = 5.344\,80$ h, was obtained by Warner (2017b) from data taken on 2016 November 30 and December 5.

The photometric spectrum of (489337) 2006 UM was derived from observations performed on 2016 December 2, and is shown in Fig. 6, normalized to the r filter. In the figure, the black dots are

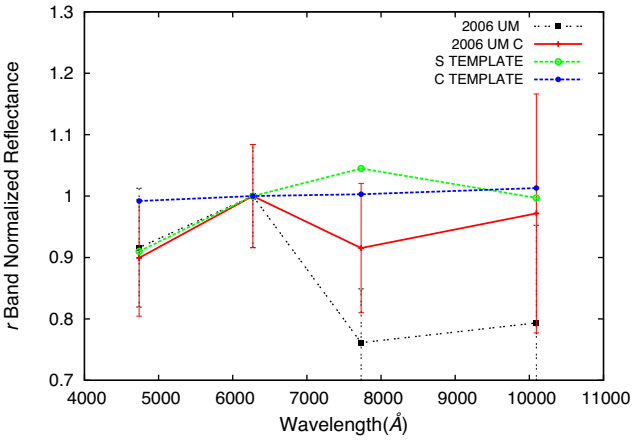

Figure 6. Photometric spectrum, normalized to the *r* filter, of asteroid (489337) 2006 UM. The points indicate the magnitude, and respective error, at the band centre for each filter. The diverse lines indicate the observed spectrum (black dotted line), the rotationally corrected spectrum (red solid line) and the templates of the S (green dashed line) and C (blue dashed line) taxonomic classification from Carvano et al. (2010).

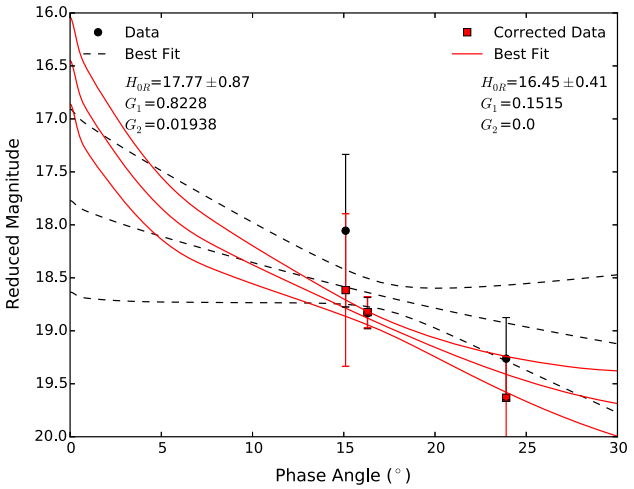

Figure 7. Phase curve for asteroid (489337) 2006 UM. The black dotted curve and red solid curve represent the fits to the observed and rotationally corrected magnitudes, respectively. In both cases the central curve represents the best fit while the error envelope is given by the upper and lower curves.

the observed magnitudes in each filter, with the respective error, while the red dots are the magnitudes corrected for the lightcurve amplitude. Although this correction substantially changes the magnitudes, the resulting reflectance spectrum is not similar to any taxonomic template of Carvano et al. (2010). Taking into account the large errors in the observed magnitudes, this spectrum can be considered compatible with the C-class.

The phase curve for asteroid (489337) 2006 UM contains just a few magnitudes taken on 2016 November and over a very limited solar phase range. These are shown in Fig. 7, where the observed and corrected magnitudes are indicated by black and red points, respectively. The best fit to each data set give quite different values for the absolute magnitudes, i.e. $H_{0R} = 17.77 \pm 0.87$ and $H_{0R} = 16.45 \pm 0.41$. Obviously, the large error envelopes are to be attributed to the small range in solar phase angles, and far from the opposition, covered by the data. It is to be noted, however, that these

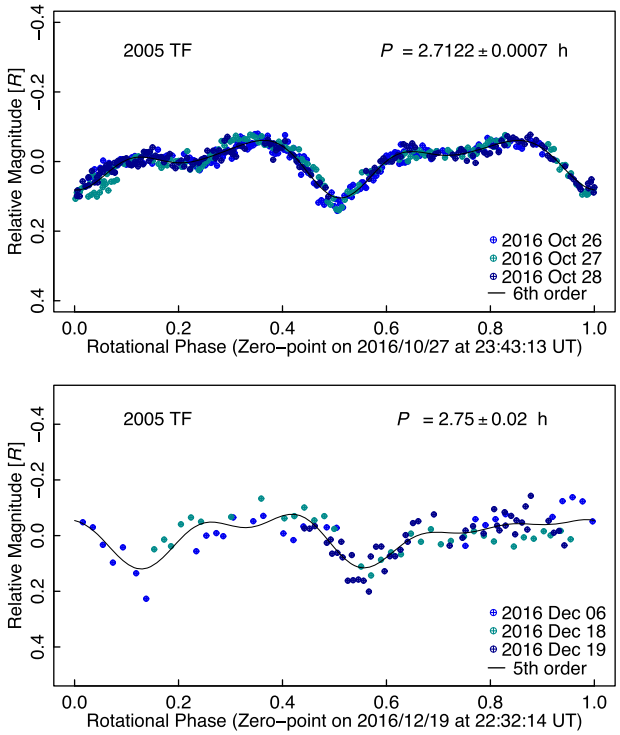

Figure 8. Composite lightcurve for 2005 TF with the best Fourier fit (black line). The upper and lower panels show data obtained at OASI and OANLH, respectively.

are quite reduced when correcting the magnitudes for the asteroid rotation.

If we assume a C-type taxonomic classification for this NEO, we can assume an albedo $\rho_v = 0.059 \pm 0.073$, which is the mean value of the class as given by Mainzer et al. (2011). Then, using the obtained colour $V - R = 0.429 \pm 0.110$, we can compute an effective diameter of $\bar{D} = 2.26$ for this asteroid, but due to the uncertainties on the taxonomic classification the obtained diameter is just indicative.

4.1.3 2005 TF

This asteroid was the only one of our sample for which lightcurves were obtained both at OASI, from 2016 October 26–28, and at OANLH, on 2016 December 6, 18 and 19. The OASI observations were fitted by a sixth-order Fourier series yielding a rotation period of $P = 2.7122 \pm 0.0007$ h with a composite lightcurve amplitude of $A = 0.166$ mag (Fig. 8). The OANLH observations were fitted by a fifth-order Fourier series deriving a period of $P = 2.75 \pm 0.02$ and amplitude of $A = 0.21$. Similar values were obtained by Vaduvescu et al. (2017), $P = 2.724 \pm 0.005$ h and $A = 0.22$, from observations on 2016 November 14. Slightly different values were derived by Warner (2017a), $P = 2.57 \pm 0.005$ h and $A = 0.29$, from observations on 2016 September 28–30 and October 1–2. The small variations among the diverse determinations might be attributed to the small amplitude of the lightcurves and the large scattering in the observed magnitudes.

The photometric spectrum for 2005 TF was determined using observations acquired on 2016 October 24 and is shown in Fig. 9. In the figure, the diverse lines represent the observed (dotted black) and the rotation-corrected (solid red) spectra along with templates of S- and V-types from Carvano et al. (2010) (dotted green and blue,

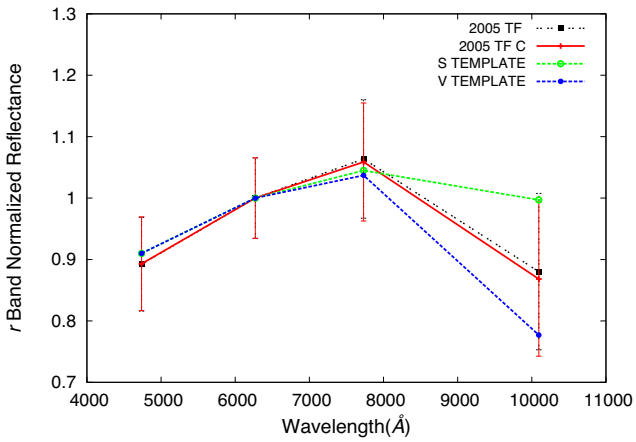

Figure 9. Photometric spectrum normalized to the r filter of the NEO 2005 TF. The points indicate the magnitude, and respective error, at the band centre for each filter. The diverse lines indicate the observed spectrum (black dotted line), the rotationally corrected spectrum (red solid line) and the templates of the S- (green dashed line) and V-type (blue dashed line) taxonomic classification from Carvano et al. (2010).

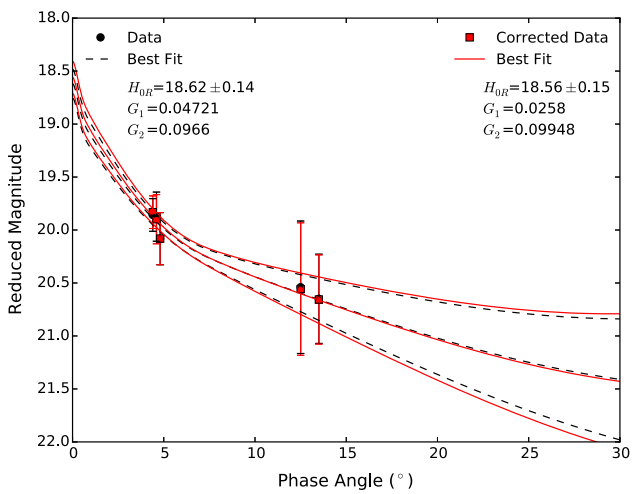

Figure 10. Phase curve of the asteroid 2005TF. The black dotted curve represents the fit to the observed magnitudes and the red solid curve that to the rotationally corrected magnitudes. In both case the central curve is the best fit to the data and the upper and lower curves represent the error envelope.

respectively). It is possible to note that the observed and corrected magnitudes do not change significantly due to the small amplitude of the rotational lightcurve. The chi-squared test indicates that the V-type best fits the obtained corrected spectrum.

The phase curve for this NEO was derived from observations performed at OASI over several nights in 2016 December, when the solar phase angle of the asteroid spanned a range from 4.4–13.5 degrees. The obtained magnitudes were corrected by rotation although this resulted in tiny variations due to the small amplitude of the lightcurve.

In Fig. 10 we show the obtained and corrected magnitudes for 2005 TF that give $H_{0R} = 18.62$, $G_1 = 0.047\,21$ and $G_2 = 0.0966$. It should be noted that, due to the small amplitude of the lightcurve, these values do not change significantly when using rotationally corrected magnitudes.

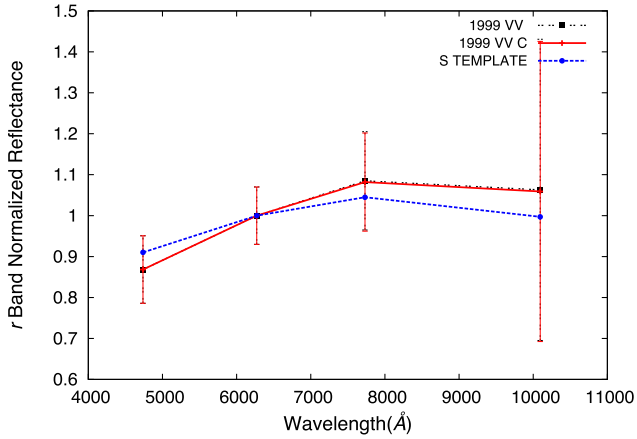

Figure 11. Photometric spectrum, normalized to the r filter, of the NEO (36236) 1999 VV. The points indicate the magnitude, and respective error, at the band centre for each filter. The diverse lines indicate the observed spectrum (black dotted line), the rotationally corrected spectrum (red solid line) and the template of the S-type (blue dashed line) taxonomic classification from Carvano et al. (2010).

Finally, to determine the effective diameter of the asteroid we first compute the colour $V - R = 0.434 \pm 0.085$ from our SDSS colours. Then, considering an albedo of $\rho_V = 0.350 \pm 0.109$, which is the mean value for the V class as given by Mainzer et al. (2011), we derive the value of $\bar{D} = 0.361 \pm 0.095$ km.

4.2 NEOs of the Apollo group

4.2.1 (36236) 1999 VV

The photometric spectrum for (36236) 1999 VV was obtained with observations performed on 2016 November 27. To perform the correction for the rotation, however, we used data available in the Asteroid Lightcurve Photometry Database (ALCDEF)[5] since it was not possible to derive the lightcurve from our observations. This lightcurve was obtained from data acquired on 2016 November 22, 23 and 25, i.e. on nights very near those of our observations. We thus used the values of $P = 6.191 \pm 0.02$ h and $A = 0.132$ mag as derived by Warner (2017b).

In Fig. 11 are given the observed and corrected magnitudes (black and red dots), which are very similar due to the small amplitude of the composite rotational lightcurve. The best fit is obtained for a template of the S-type taxonomic class, which is shown by the blue dotted line.

The phase curve for this asteroid was determined from observations obtained during several nights on 2016 November and December, spanning phase angles from 7.6 to 13 degrees. In Fig. 12 are shown the obtained magnitudes along with the best fit, which give the values $H_{0R} = 15.77 \pm 0.03$, $G_1 = 0.8228$ and $G_2 = 0.019\,38$.

The effective diameter, $\bar{D} = 1.615 \pm 0.370$, for asteroid (36236) 1999 VV was computed from equation (11) using the determined colour $V - R = 0.416 \pm 0.094$ and the absolute magnitude H_{0R}, as well as the average albedo for the S taxonomic class (Mainzer et al. 2011).

[5] http://alcdef.org

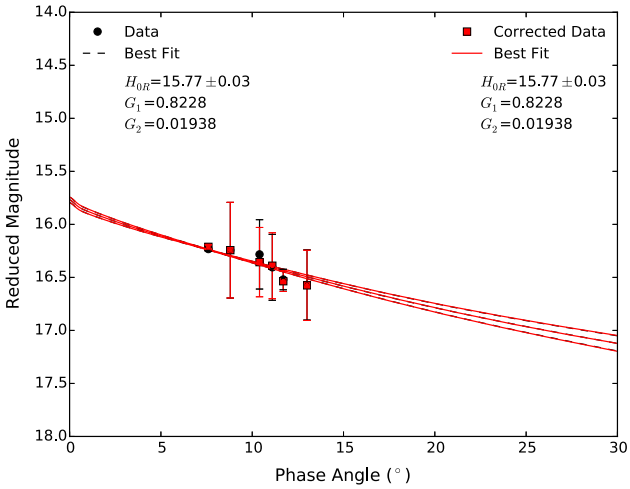

Figure 12. Phase curve of the asteroid (36236) 1999 VV. The black dotted curve represents the fit to the observed magnitudes and the red solid curve that to the rotationally corrected magnitudes. In both cases the central curve is the best fit to the data and the upper and lower curves represent the error envelope.

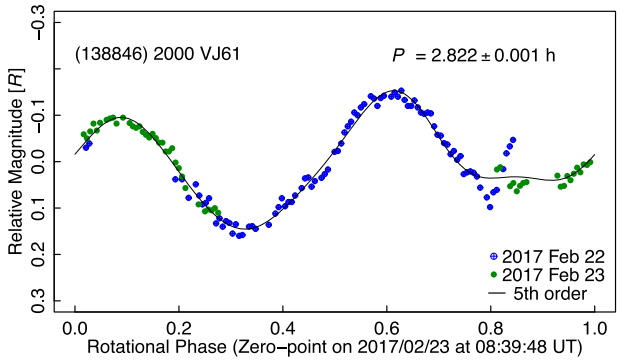

Figure 13. Composite lightcurve for the NEO (138846) 2000 VJ61, showing the best Fourier fit (black line).

4.2.2 (138846) 2000 VJ61

We observed this NEO on 2017 February 22 and 23 to derive its lightcurve. The obtained data were fitted by a fifth-order Fourier series, deriving a rotation period of $P = 2.822 \pm 0.01$ h and a composite lightcurve amplitude of $A = 0.30$ mag, as shown in Fig. 13. Erasmus et al. (2017) reported this asteroid as a rapid rotator with a period $P = 1.29$ h, derived from data obtained over 1.13 h on 2017 February 12. We tried to fit this period to our data, but without success. The good fit to the data with a period of about 2.8 h seems to confirm that our value is the correct one.

The photometric spectrum for this asteroid was determined using magnitudes obtained on 2016 December 6. The magnitudes were corrected to account for the rotational variations as given by the lightcurve (Fig. 13), since the lightcurve amplitude is appreciable. In Fig. 14 are given the observed and corrected magnitudes as well as the derived spectra. Comparing the obtained spectrum with diverse templates of the Carvano et al. (2010) taxonomic scheme, the best fit was obtained for the Q-type class, although the S class cannot be excluded. Although Carry et al. (2016) classify this asteroid as a C-type, analysis of their data indicates that an S-type class cannot be ruled out, since the error in the z filter is quite large, as in our spectrum. Moreover, these authors do not take into account

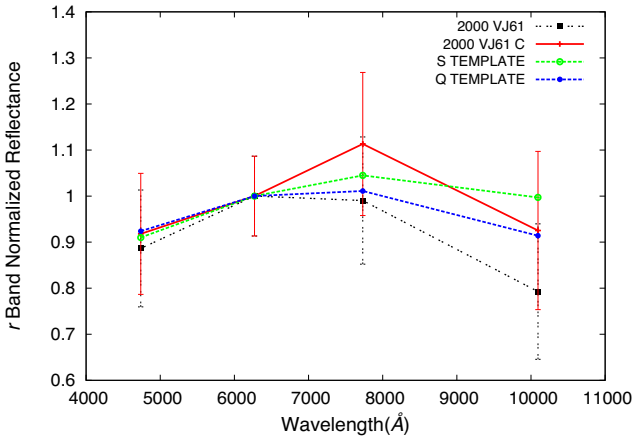

Figure 14. Photometric spectrum normalized to the r filter of the NEO (138846) 2000 VJ61. The points indicate the magnitude, and respective error, at the band centre for each filter. The diverse lines indicate the observed spectrum (black dotted line), the rotationally corrected spectrum (red solid line) and the templates of the S- (green dashed line) and Q-type (blue dashed line) taxonomic classification from Carvano et al. (2010).

Table 1. Summary of the physical parameters derived for each observed NEO.

Asteroid	P (h)	A	Tx	$V-R$	H_{0R}
Amor Group					
(326683) 2002 WP	6.261	1.33	A	0.486	16.97
(489337) 2006 UM	5.344	1.191	C?	0.429	16.45
2005 TF	2.7122	0.22	V	0.434	18.56
Apollo Group					
(36236) 1999 VV	6.191	0.132	S	0.452	15.77
(138846) 2000 VJ61	2.822	0.30	Q	0.416	14.89
2016 WJ1	2.944	0.116	–	–	20.98

Asteroid	H_0	G_1	G_2	$\bar{D}$(km)
Amor Group				
(326683) 2002 WP	17.46	0.164	0.010 05	0.771
(489337) 2006 UM	16.88	0.1515	0.0	2.262
2005 TF	18.99	0.0258	0.099 48	0.361
Apollo Group				
(36236) 1999 VV	16.22	0.8228	0.019 38	1.615
(138846) 2000 VJ61	15.306	–	–	–
2016 WJ1	–	0.2588	0.3721	–

P = period, A = amplitude, Tx = taxonomic class, $V-R$ = colour
H_{0R} = absolute magnitude in the R filter
H_0 = absolute magnitude in the V filter
$G_1 - G_2$ = slope parameters
$\bar{D}$ = effective diameter

the amplitude of the lightcurve, which in this case can be large, substantially modifying the spectrum and the classification. It must be noted that Erasmus et al. (2017) classify this asteroid as S-type, with a high probability (0.81) of belonging to this class. Anyhow, we believe that new observations are necessary to firmly establish the taxonomic classification of this asteroid as well as to verify the existence of compositional variations on its surface. The obtained magnitudes also allowed derivation of the colour $V-R = 0.416 \pm 0.136$ for this object.

Magnitudes in the R-Cousins filter were obtained for this NEO on some nights in 2016 November and December, spanning a very limited interval of solar phase angles and far from opposition: from

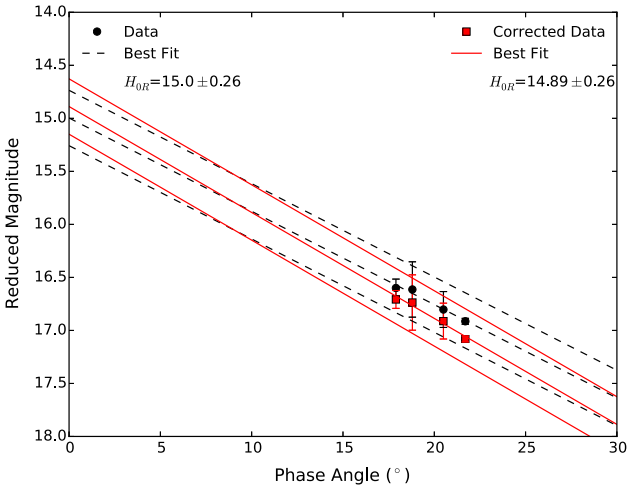

Figure 15. Phase curve of the asteroid (138846) 2000 VJ61. The black dotted curve represents the fit to the observed magnitudes and the red solid curve that to the rotationally corrected magnitudes. In both cases the central curve indicates the best fit to the data and the upper and lower curves represent the error envelope.

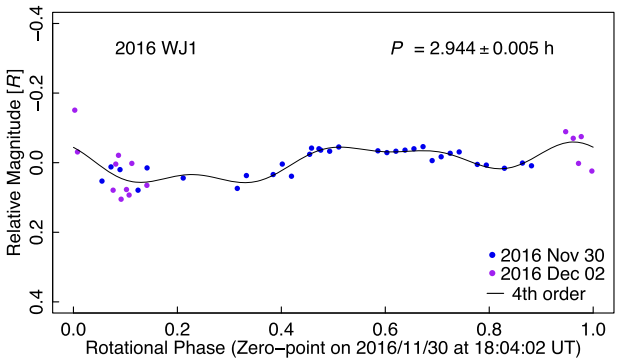

Figure 16. Composite lightcurve of the NEO 2016 WJ1, showing the best fit (black line).

17.9 to 21.7 degrees. The obtained phase curve is given in Fig. 15 in which are shown the observed magnitudes as well as those corrected by the rotation. Due to the very limited interval in phase angles, the absolute magnitude was obtained by a linear fit to the corrected data, giving a value of $H_{0R} = 14.89$ (Fig. 15, solid red curve). The large uncertainty on the absolute magnitude did not allow us to derive an effective diameter for this asteroid.

4.2.3 2016 WJ1

To derive the rotation period for asteroid 2016 WJ1, we performed observations on 2016 November 30 and December 2. The obtained data were fitted by a fourth-order Fourier series, giving a rotation period of $P = 2.944 \pm 0.05$ h and composite lightcurve amplitude of $A = 0.116$ mag (Fig. 16). Erasmus et al. (2017), from observations over 1.783 h on 2016 November 29, concluded that this asteroid is a rapid rotator with $P = 20$ min. This result was not confirmed by Warner (2017b), which derived a period of $P = 2.68$ h with observations obtained from 2016 November 28–30. Although this value is very similar to ours, the small amplitude of the composite lightcurve makes it more difficult to derive the period. We believe

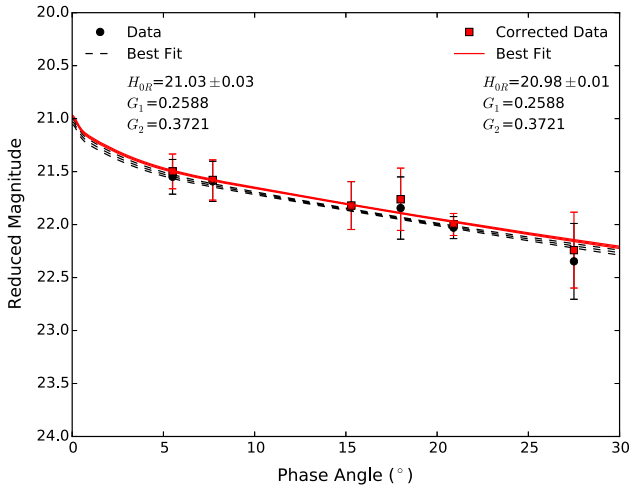

Figure 17. Phase curve of the asteroid 2016 WJ1. The black dotted curve represents the fit to the observed magnitudes and the red solid curve that to the rotationally corrected magnitudes. In both cases the central curve indicates the best fit to the data and the upper and lower curves represent the error envelope.

that new observations are necessary to establish with precision the rotation period for this asteroid.

Observations of this asteroid over several nights in 2016 November and December enabled us to obtain magnitudes, in the *R*-Cousins filter, between 5.5 and 27.5 degrees in solar phase angles, the largest range in the present work. In Fig. 17 are shown the observed magnitudes and their best fit, indicated by black dots and lines. Due to the small amplitude of the composite lightcurve, the corrected magnitudes (in red) show minor variations. The derived absolute magnitude is $H_{0R} = 20.98 \pm 0.01$ and the slope parameters are $G_1 = 0.2588$ and $G_2 = 0.3721$.

For this asteroid, photometric observations were attempted on 2016 December 2 and 5, but the atmospheric conditions were poor on the first night, and the asteroid was very near a bright star on the second. Therefore, we were unable to derive the taxonomic type and the effective diameter for the NEO 2016 WJ1.

5 DISCUSSION AND CONCLUSIONS

We obtained a set of physical parameters for six NEOs, i.e. three of the Amor and three of the Apollo groups. For each asteroid we performed observations on almost consecutive nights to accompany the brightness variations with rotation, wavelength and solar illumination. To achieve this goal, for each selected asteroid, we construct the lightcurve, the photometric spectra, and the phase curve. The results are summarized in Table 1, where for each NEO is given: the rotation period, P; the amplitude of the composite lightcurve at the time of observations, A; the taxonomic class, Tx; the colour $(V - R)$; the absolute magnitude in the R filter, H_{0R}; the absolute magnitude in the V filter, H_0; the slope parameters, $G1 - G2$; and the effective diameter $\bar{D}$.

We note that all the observed NEOs have rotation periods in a range from 2.7–6.2 h and the corresponding lightcurves have amplitudes between 0.116 and 1.3 mag. These values were used to correct the magnitudes of the photometric spectra and the phase curves for each NEO. The present results confirm that these corrections are in fact very relevant, in particular when the amplitude is large. In the case of asteroids (489337) 2006 UM and (326683)

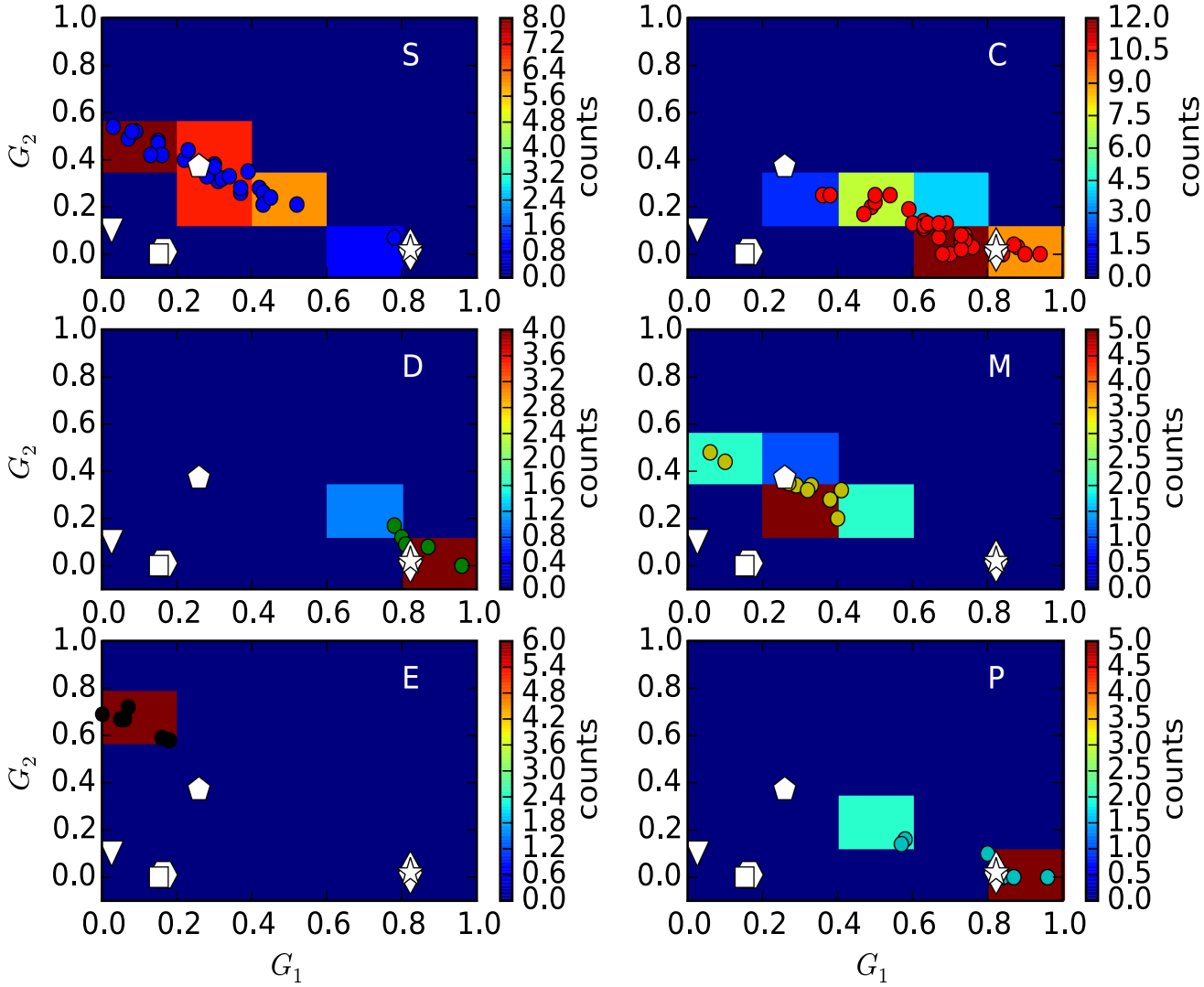

Figure 18. Bidimensional histogram of the slope parameters G_1, G_2 in different taxonomical classes for the sample of 93 main-belt asteroids given in Shevchenko et al. (2016). The positions of our objects are indicated by the following large white symbols: hexagon, (326683) 2002 WP; square, (489337) 2006 UM; triangle, 2005 TF; diamond, (36236) 1999 VV; star, (138846) 2000 VJ61; and pentagon, 2016 WJ1.

2002 WP, for example, the error in the absolute magnitude decreased from 0.87 to 0.41 mag and from 0.29 to 0.05 mag, respectively. Thus, not correcting the magnitudes to account for the rotational variations of the asteroid can lead to unrealistic physical parameters.

Among the six studied asteroids, we have determined their taxonomic classifications with significant confidence, with three of the S-complex, (36236) 1999 VV, (138846) 2000 VJ61 and (326683) 2002 WP, and one of the V-type, 2005 TF. Note that these classifications are consistent with Erasmus et al. (2017), where (326683) 2002 WP and (138846) 2000 VJ61 are classified as S-type. In the case of asteroid (489337) 2006 UM, the large errors in the magnitudes, especially in the z filter, do not allow for a firm classification. Although the best fit within the classification scheme of Carvano et al. (2010) is the C-type template, other classifications cannot be ruled out.

In order to examine our values of slope parameter within the taxonomic classification approach, we plotted them in the phase space $G_1 \times G_2$, together with those of 93 main-belt asteroids of different classes given by Shevchenko et al. (2016), as shown in Fig. 18. In this figure the 93 main-belt asteroids are shown by coloured dots separately in the respective plots, S, C, D, M, E and P, according to the taxonomic classification attributed to Shevchenko et al. (2016). The coloured rectangles indicate the population density. The NEOs studied in the present work are shown in white symbols. According to these plots, the three asteroids of the Amor group do not fit within any region, in any taxonomic class, and, more importantly, do not even follow the linear trend shown by the data in Shevchenko et al. (2016). For the three asteroids of the Apollo group, we can observe that asteroid 2016 WJ1 can be classified as S-type or M-type (of the X-complex) while (36236) 1999 VV and (138846) 2000 VJ61 are D-, C- or P-type and even S-type, where all these asteroids follow the linear trend showed by Shevchenko et al. (2016). For asteroid 2016 WJ1 we do not have a photometric spectrum in order to compare, but Erasmus et al. (2017) classified this object as X-type, this being one of the possibilities given by the $G_1 - G_2$ values. For asteroid (36236) 1999 VV, the obtained spectrum (Fig. 11) seems to be compatible with an S-type. However, due to the large errors in the z filter, a D-type classification cannot be ruled out. For asteroid (138846) 2000 VJ61, the obtained spectrum can be best fitted by a Q-type template (note that this

Table 2. Probability of each observed asteroid belonging to a given taxonomic class having specific values $G_1 - G_2$.

Asteroid	$\mathcal{P}_{SG_1G_2}$	$\mathcal{P}_{CG_1G_2}$	$\mathcal{P}_{DG_1G_2}$	$\mathcal{P}_{MG_1G_2}$	$\mathcal{P}_{EG_1G_2}$	$\mathcal{P}_{PG_1G_2}$
Amor Group						
(326683) 2002 WP	0	0	0	0	0	0
(489337) 2006 UM	0	0	0	0	0	0
2005 TF	0	0	0	0	0	0
Apollo Group						
(36236) 1999 VV	0	0.016	0.029	0	0	0.014
(138846) 2000 VJ61	0	0.016	0.029	0	0	0.014
2016 WJ1	0.018	0	0	0.0097	0	0

class is part of the S-complex). Using the values of $G_1 - G2$ given in Fig. 18, we observe that in the Shevchenko et al. (2016) sample there is just one object of the S-complex with values similar to the ones obtained here.

We further computed the probability of an asteroid belonging to a given spectral type and having specific values of G_1 and G_2. This was done using equation (12), where $\mathcal{P}_X$ is the probability of the asteroid having a specific taxonomy type, $\mathcal{P}_{G_1G_2}$ is the probability of having values $G1$ and $G2$ inside a specific bin, $\mathcal{N}_\mathcal{X}$ is the number of asteroids in a specific taxonomy class, $\mathcal{N}_\mathcal{T}$ is the total number of asteroids in the sample of Shevchenko et al. (2016), and $\mathcal{N}_{G_1G_2}$ is the number of particles inside a specific bin.

In Table 2 we can observe that the three asteroids of the Amor group have zero probability of belonging to one of the taxonomic classes showed by Shevchenko et al. (2016). Among the Apollo group, two NEOs, (36236) 1999 VV and (138846) 2000 VJ61, have a higher probability of belonging to the D class and 2016 WJ1 to the S class. For these asteroids, however, the probability of belonging to another taxonomic class is not null. Although this analysis confirms the result obtained from Fig. 18, the results are intriguing. It is to be noted that for the Amor asteroids we have good photometric spectra for two of them: (326683) 2002 WP and 2005 TF, classified as S-type and V-type, respectively. However, the above analysis fails for both asteroids. We can speculate that this is due to the different size ranges of our sample and that of Shevchenko et al. (2016). It is noteworthy that the $G_1 - G_2$ values given by this author are for main-belt asteroids, which are much larger than those studied here:

$$\mathcal{P}_{XG_1G_2} = \mathcal{P}_X \mathcal{P}_{G_1G_2} = \left(\frac{\mathcal{N}_\mathcal{X}}{\mathcal{N}_\mathcal{T}}\right)\left(\frac{\mathcal{N}_{G_1G_2}}{N_X}\right)^2. \quad (12)$$

The first conclusion that we can derive from the above analysis is that the number of objects with good slope parameters and taxonomic classification among the NEO population continues to be very small. Projects like the IMPACTON are therefore very important to increase the sample of NEOs with reliable physical parameters and thus to better understand this very intriguing population. The second conclusion regards the importance of performing a complete photometric characterization in order to derive reliable physical properties. As we have clearly shown, all the physical parameters are related and we cannot derive one without taking into account the others. An obvious example is the photometric magnitude of an asteroid, which depends on the brightness variations due to its shape.

Last but not least, it is noteworthy that among the five NEOs for which a photometric spectrum was obtained and a taxonomic classification was possible, four belong to the S-complex. Erasmus et al. (2017) use photometry on the Johnson–Cousins filters to derive the taxonomic classification for a sample of 39 NEOs, and report that the number of S-type NEOs appears to be similar to that of the C-complex (plus D and X classes). This result seems not to be in agreement with the work by Carry et al. (2016), which classifies 206 NEOs from SDSS colours, as well as with theoretical works (e.g. Bottke et al. 2002; Greenstreet, Ngo & Gladman 2012), which indicate a greater flux of NEOs from the inner main belt, where there is a majority of S-type asteroids. Differences among the diverse samples and the methodologies used to derive the results might account for the discrepancies in the results but the important point is that only a much larger data set of NEOs with reliable physical parameters will allow this interesting population to be better constrained.

ACKNOWLEDGEMENTS

ER, PA, FM and HM would like to thank CNPq and CAPES for their support through diverse fellowships. Support by CNPq (305409/2016-6) and FAPERJ (E-26/202.841/2017) is acknowledged by DL. The authors are grateful to the IMPACTON team, in particular to R. Souza and A. Santiago for the technical support. Observations were obtained at the Observatório Astronômico do Sertão de Itaparica (OASI, Itacuruba) of the Observatório Nacional (ON-Brazil), with complementary observations from the Observatorio Astronómico Nacional Llano del Hato operated by Centro de Investigaciones de Astronomía (CIDA-Venezuela).

REFERENCES

Bottke W. F., Morbidelli A., Jedicke R., Petit J.-M., Levison H. F., Michel P., Metcalfe T. S., 2002, Icarus, 156, 399
Bowell E., Lumme K., 1979, in Gehrels T., Matthews M. S., eds, Asteroids, University of Arizona Press, Tucson. p. 132
Bowell E., Hapke B., Domingue D., Lumme K., Peltoniemi J., Harris A. W., 1989, in Binzel R. P., Gehrels T., Matthews M. S., eds, Asteroids II, University of Arizona Press, Tucson. p. 524
Carry B., Solano E., Eggl S., DeMeo F. E., 2016, Icarus, 268, 340
Carvano J. M., Hasselmann P. H., Lazzaro D., Mothé-Diniz T., 2010, A&A, 510, A43
Ditteon R. et al., 2018, Minor Planet Bull., 45, 13
Erasmus N., Mommert M., Trilling D. E., Sickafoose A. A., van Gend C., Hora J. L., 2017, AJ, 154, 162
Fowler J., Chillemi J., 1992, Tedesco, IRAS asteroid data processing. Vol. 17, Tech. Rep., Hanscom Air Force Base, MA, Phillips Laboratory, Phillips Laboratory, Hanscom Air Force Base, Massachusetts
Gehrels T., Coffeen T., Owings D., 1964, AJ, 69, 826
Greenstreet S., Ngo H., Gladman B., 2012, Icarus, 217, 355
Hapke B., 1990, Icarus, 88, 407
Hapke B., 1993, Theory of Reflectance and Emittance Spectroscopy, Cambridge University Press, Cambridge
Hapke B., 2002, Icarus, 157, 523
Harris A. W. et al., 1989, Icarus, 77, 171

Harris A. W., Lagerros J. S. V., 2002, in, Bottke W., Cellino A., Paolicchi P., eds, in Asteroids in the Thermal Infrared, University of Arizona Press, Tucson, p. 205
Howell S. B., 1989, PASP, 101, 616
Kaasalainen M. et al., 2004, Icarus, 167, 178
Lumme K., Bowell E., 1981, AJ, 86, 1694
Lupton R., 2005, Transformations between SDSS magnitudes and UBVRcIc , Available at: http://www.sdss.org/dr4/-algorithms/sdssUBVRITransform.html
Mainzer A. et al., 2011, ApJ, 741, 90
Mainzer A. K. et al., 2016, NASA Planetary Data System, 247EAR
Mommert M. et al., 2016, AJ, 151, 98
Muinonen K., Belskaya I. N., Cellino A., Delbò M., Levasseur-Regourd A.-C., Penttilä A., Tedesco E. F., 2010, Icarus, 209, 542
Penttilä A., Shevchenko V. G., Wilkman O., Muinonen K., 2016, Planet. Space Sci., 123, 117
Perna D. et al., 2017, A&A, 599, L1
Pravec P., Šarounová L., Wolf M., 1996, Icarus, 124, 471
Pravec P., Wolf M., Šarounová L., 1998, Icarus, 136, 124
Seeliger H., 1887, Zur Theorie der Beleuchtung der grossen Planeten insbesondere des Saturn. Aus den Abhandlungen der k. bayer. Akademie der Wiss. II Cl. 16 Bd. II Abth. Verlag der k. Akademie in Comm. bei G. Franz, Bayer Akademie der Wissenschaften, Munich, Germany
Shevchenko V. G. et al., 2016, Planet. Space Sci., 123, 101
Thorpe T. E., 1978, Icarus, 36, 204
Vaduvescu O. et al., 2017, Earth Moon Planets, 120, 41
Verbiscer A. J., Veverka J., 1995, Icarus, 115, 369
Warner B. D., 2017a, Minor Planet Bull., 44, 22
Warner B. D., 2017b, Minor Planet Bull., 44, 98
Warner B. D., Harris A. W., Pravec P., 2009, Icarus, 202, 134
Whiteley R. J., Tholen D. J., Hergenrother C. W., 2002, Icarus, 157, 139
Zappala V., Cellino A., Barucci A. M., Fulchignoni M., Lupishko D. F., 1990, A&A, 231, 548

APPENDIX A: ADDITIONAL TABLES

In what follows are given the observational circunstances and the derived parameters described in the paper. In Table A1 are given the values of the Fourier series of the composite rotational lightcurve for each observed asteroid. The observational circumstances of the data obtained to derived the rotational lightcurves, the photometric spectra and the phase curves are given in Tables A2, A3 and A4 respectively.

Table A1. Fourierseries coefficients. Columns A1–A6 are the sine terms and B1–B6 are the cosine terms of the Fourier model for the lightcurve. The order of best fits is given by the number of coefficients.

Asteroid	A1	B1	A2	B2	A3	B3	A4	B4	A5	B5	A6	B6
Amor Group												
(326683) 2002 WP	0.003 83	0.012 03	0.579 25	0.028 06	− 0.002 73	0.010 84	0.023 24	− 0.180 89	0.000 58	− 0.006 71	− 0.078 56	− 0.012 07
(489337) 2006 UM	− 0.008 87	0.003 28	0.494 42	0.060 19	− 0.056 71	0.014 57	0.044 45	− 0.084 97	0.017 82	0.015 71	− 0.027 15	− 0.031 55
2005 TF (OASI)	0.0048	− 0.002 85	0.022 17	0.046 86	− 0.005 48	− 0.006 57	− 0.001 23	0.037 91	− 0.003 04	− 0.000 91	0.002 16	0.007 13
2005 TF (CIDA)	0.0032	− 0.0086	0.063	0.012	− 0.0046	− 0.029	0.02	− 0.016	− 0.026	− 0.011	–	–
Apollo Group												
(36236) 1999 VV	–	–	–	–	–	–	–	–	–	–	–	–
(138846) 2000 VJ61	0.022 50	0.012 45	− 0.006 52	− 0.076 60	− 0.045 96	0.044 50	− 0.014 46	0.004 57	− 0.014 48	0.012 41	–	–
2016 WJ1	0.006 80	0.017 58	0.017 64	− 0.018 86	0.007 57	− 0.026 88	0.006 93	0.008 43	–	–	–	–

Table A2. Observational circumstances of the rotational lightcurve data. For each asteroid is given: the name, the observation interval, the number of images used, the total span of time of the observations, the distance to the Earth (Δ) and to the Sun (r), the solar phase angle (α), the apparent $\overline{V}$ magnitude and the observatory where the data were acquired. The values of Δ, r, α and $\overline{V}$ are given for the start date.

Asteroid	Date	Images used	Observed time (h)	Δ (au)	r (au)	α (°)	$\overline{V}$	Observatory
Amor Group								
(326683) 2002 WP	2016/11/26–2016/11/29	466	8.0	0.169	1.142	22.2	15.9	OASI
(489337) 2006 UM	2016/12/02–2016/12/04	379	7.5	0.190	1.149	28.8	16.4	OASI
2005 TF	2016/10/26–2016/10/29	548	11.0	0.143	1.137	4.5	16.7	OASI
	2016/12/06–2016/12/19	112	8.0	0.103	1.072	31.6	16.8	CIDA
Apollo Group								
(138846) 2000 VJ61	2017/02/22–2017/02/23	143	4.5	0.420	1.118	61.7	16.5	OASI
2016 WJ1	2016/11/30–2016/12/02	47	4.0	0.133	1.117	11.0	17.8	OASI

Table A3. Observational circumstances and derived magnitudes of the photometric spectra. For each asteroid is given: the name, the date and start time, the filter, the calibrated magnitude (mag) and its error (Δmag), the averaged magnitude ($\overline{\text{mag}}$) and its error ($\Delta\overline{\text{mag}}$), the averaged magnitude corrected by rotation ($\overline{\text{mag}_c}$) and its error ($\Delta\overline{\text{mag}_c}$), and the solar phase angle (α) at the start instant.

Asteroid	Date	UT	Filter	mag	Δmag	$\overline{\text{mag}}$	$\Delta\overline{\text{mag}}$	$\overline{\text{mag}_c}$	$\Delta\overline{\text{mag}_c}$	α (°)
(326683) 2002 WP	2016/11/27	04:29:27.11	*g*	16.2255	0.014	16.602	0.017 6429	16.532	0.017 6429	21.9
	2016/11/27	04:36:51.02	*g*	16.301	0.016					
	2016/11/27	04:44:14.44	*g*	16.4155	0.016					
	2016/11/27	04:51:38.49	*g*	16.5565	0.017					
	2016/11/27	04:59:02.28	*g*	16.6755	0.0185					
	2016/11/27	05:06:35.08	*g*	16.9095	0.019					
	2016/11/27	05:14:00.74	*g*	17.1305	0.023					
	2016/11/27	04:27:50.22	*r*	15.5205	0.011	15.8835	0.013 6429	15.8835	0.013 6429	
	2016/11/27	04:35:13.24	*r*	15.5945	0.0115					
	2016/11/27	04:42:36.89	*r*	15.6735	0.012					
	2016/11/27	04:50:00.91	*r*	15.827	0.0135					
	2016/11/27	04:57:24.61	*r*	15.9585	0.014					
	2016/11/27	05:04:58.11	*r*	16.198	0.0165					
	2016/11/27	05:12:23.02	*r*	16.4125	0.017					
	2016/11/27	04:31:01.81	*i*	15.317	0.016	15.7304	0.0205	15.6554	0.0205	
	2016/11/27	04:38:25.60	*i*	15.38	0.018					
	2016/11/27	04:45:49.00	*i*	15.5665	0.0185					
	2016/11/27	04:53:13.17	*i*	15.67	0.0195					
	2016/11/27	05:00:36.85	*i*	15.85	0.0215					
	2016/11/27	05:08:10.85	*i*	16.042	0.022					
	2016/11/27	05:15:35.36	*i*	16.2875	0.028					
	2016/11/27	04:33:05.97	*z*	15.384	0.0295	15.9136	0.055 8571	15.7136	0.055 8571	
	2016/11/27	04:40:29.81	*z*	15.505	0.035					
	2016/11/27	04:47:53.60	*z*	15.691	0.0425					
	2016/11/27	04:55:17.47	*z*	15.9195	0.053					
	2016/11/27	05:02:41.10	*z*	15.9345	0.054					
	2016/11/27	05:10:15.55	*z*	16.2935	0.0685					
	2016/11/27	05:17:40.49	*z*	16.668	0.1085					
(489337) 2006 UM	2016/12/03	01:23:04.60	*g*	16.677	0.0395	16.7756	0 .049	16.7056	0.049	28.8
	2016/12/03	01:27:40.21	*g*	16.749	0.0535					
	2016/12/03	01:30:33.48	*g*	16.8105	0.052					
	2016/12/03	01:33:27.19	*g*	16.866	0.051					
	2016/12/03	01:21:36.75	*r*	16.11	0.0435	16.2404	0.045 625	16.1504	0.045 625	
	2016/12/03	01:26:12.82	*r*	16.2465	0.0445					
	2016/12/03	01:29:05.89	*r*	16.2655	0.0475					
	2016/12/03	01:31:59.23	*r*	16.3395	0.047					
	2016/12/03	01:36:00.50	*i*	16.3185	0.055	16.4264	0.059 25	16.1364	0.059 25	
	2016/12/03	01:39:33.76	*i*	16.4225	0.062					
	2016/12/03	01:43:06.62	*i*	16.429	0.057					
	2016/12/03	01:46:40.88	*i*	16.5355	0.063					
	2016/12/03	01:37:46.07	*z*	16.445	0.1375	16.3515	0.151 75	16.0415	0.151 75	
	2016/12/03	01:41:18.82	*z*	16.3125	0.1805					
	2016/12/03	01:44:52.88	*z*	16.3765	0.127					
	2016/12/03	01:48:26.67	*z*	16.272	0.162					
2005 TF	2016/10/25	01:16:24.91	*g*	17.225	0.034	17.289	0.037 25	17.355	0.037 25	4.3
	2016/10/25	01:28:48.27	*g*	17.251	0.0345					
	2016/10/25	01:41:14.52	*g*	17.381	0.0395					
	2016/10/25	01:53:40.11	*g*	17.299	0.041					
	2016/10/25	01:14:17.97	*r*	16.6675	0.0335	16.7252	0.035 625	16.7922	0.035 625	
	2016/10/25	01:26:41.27	*r*	16.682	0.033					
	2016/10/25	01:39:06.81	*r*	16.826	0.0345					
	2016/10/25	01:51:32.58	*r*	16.7255	0.0415					
	2016/10/25	01:18:29.63	*i*	16.485	0.0425	16.5482	0.042 875	16.6202	0.042 875	
	2016/10/25	01:30:53.44	*i*	16.537	0.0435					
	2016/10/25	01:43:19.64	*i*	16.645	0.047					
	2016/10/25	01:55:46.00	*i*	16.526	0.0385					
	2016/10/25	01:22:34.67	*z*	16.641	0.102	16.7237	0.101 375	16.8057	0.101 375	
	2016/10/25	01:34:59.13	*z*	16.8885	0.101					
	2016/10/25	01:47:25.17	*z*	16.682	0.114					
	2016/10/25	01:59:50.85	*z*	16.6835	0.0885					

Table A3 – *continued*

Asteroid	Date	UT	Filter	mag	Δmag	$\overline{\text{mag}}$	$\Delta\overline{\text{mag}}$	$\overline{\text{mag}_c}$	$\Delta\overline{\text{mag}_c}$	α (°)
(36236) 1999 VV	2016/11/27	05:40:35.66	*g*	18.072	0.043	18.0729	0.045 125	18.0869	0.045 125	7.7
	2016/11/27	05:52:38.85	*g*	18.058	0.043					
	2016/11/27	06:04:43.20	*g*	18.09	0.046					
	2016/11/27	06:16:48.41	*g*	18.0715	0.0485					7.7
	2016/11/27	05:37:58.69	*r*	17.506	0.039	17.4797	0.038 125	17.4937	0.038 125	
	2016/11/27	05:50:01.77	*r*	17.4425	0.036					
	2016/11/27	06:02:05.41	*r*	17.4695	0.0375					
	2016/11/27	06:14:10.05	*r*	17.501	0.04					
	2016/11/27	05:43:10.30	*i*	17.255	0.052	17.2812	0.062 25	17.2982	0.062 25	
	2016/11/27	05:55:13.67	*i*	17.275	0.0555					
	2016/11/27	06:07:18.60	*i*	17.237	0.053					
	2016/11/27	06:19:24.16	*i*	17.358	0.0885					
	2016/11/27	05:46:34.55	*z*	18.42	0.566	17.2735	0.317 875	17.2915	0.317 875	
	2016/11/27	05:58:38.36	*z*	17.584	0.2265					
	2016/11/27	06:10:42.94	*z*	16.752	0.1455					
	2016/11/27	06:22:49.75	*z*	16.338	0.3335					
(138846) 2000 VJ61	2016/12/06	05:10:13.08	*g*	17.9216	0.088	17.992	0.0884	17.882	0.0884	17.3
	2016/12/06	05:22:23.53	*g*	18.029	0.09					
	2016/12/06	05:29:14.91	*g*	17.9972	0.088					
	2016/12/06	05:36:06.50	*g*	17.988	0.087					
	2016/12/06	05:40:35.75	*g*	18.0241	0.089					
	2016/12/06	05:06:45.77	*r*	17.3218	0.047	17.421	0.047	17.349	0.047	
	2016/12/06	05:25:47.86	*r*	17.4733	0.048					
	2016/12/06	05:32:39.42	*r*	17.4678	0.046					
	2016/12/06	05:45:06.88	*i*	17.2521	0.083	17.3216	0.0845	17.1226	0.0845	
	2016/12/06	05:53:18.70	*i*	17.3359	0.086					
	2016/12/06	06:01:31.17	*i*	17.3443	0.084					
	2016/12/06	06:09:44.17	*i*	17.3543	0.085					
	2016/12/06	05:49:11.25	*z*	17.3165	0.123	17.5333	0.1345	17.2933	0.1345	
	2016/12/06	05:57:23.20	*z*	17.603	0.143					
	2016/12/06	06:05:36.41	*z*	17.761	0.14					
	2016/12/06	06:13:49.00	*z*	17.4526	0.132					

Table A4. Observational circumstances and derived magnitudes of the phase curves. For each asteroid is given: the name, the date and start time, the instrumental magnitude (M_{obs}), the reduced magnitude (M_{red}), the averaged reduced magnitude ($\overline{M_{red}}$), the reduced magnitude corrected for the rotation (M_{cor}), the averaged reduced magnitude corrected for the rotation ($\overline{M_{cor}}$), the error of the reduced magnitude (ΔM), the averaged error of the relative magnitude ($\overline{\Delta M}$), the distance to the Earth (Δ) and to the Sun (r), and the solar phase angle (α).

Asteroid	Date	UT	M_{obs}	M_{red}	$\overline{M_{red}}$	M_{cor}	$\overline{M_{cor}}$	ΔM	$\overline{\Delta M}$	Δ (au)	r (au)	α (°)
(326683) 2002 WP	2016/11/27	04:16:41.92	16.982	18.612	18.780	19.517	19.636	0.139	0.139	0.169	1.141	21.9
		04:18:15.72	16.981	18.859		19.693		0.139				
		04:19:50.00	16.987	18.865		19.699		0.139				
	2016/12/03	04:43:28.00	16.809	18.751	18.778	18.788	18.811	0.247	0.249	0.156	1.138	10.7
		04:44:52.19	16.830	18.771		18.808		0.248				
		04:46:16.83	16.844	18.784		18.821		0.249				
		04:47:40.88	16.867	18.807		18.827		0.250				
	2016/12/04	03:18:21.45	17.607	19.605	19.637	18.697	18.729	0.240	0.240	0.154	1.138	8.8
		03:19:15.94	17.643	19.640		18.732		0.240				
		03:20:10.56	17.640	19.637		18.729		0.240				
		03:21:04.49	17.669	19.666		18.758		0.240				
	2016/12/05	03:35:17.19	16.549	18.521	18.529	18.521	18.540	0.078	0.078	0.153	1.138	6.9
		03:36:21.44	16.554	18.526		18.526		0.078				
		03:37:25.53	16.569	18.541		18.563		0.078				
(489337) 2006 UM	2016/11/24	00:10:14.17	17.425	18.057	18.055	18.594	18.615	0.722	0.720	0.221	1.199	15.1
		00:11:58.41	17.417	18.055		18.591		0.721				
		00:13:42.39	17.412	18.049		18.585		0.720				
		00:15:27.17	17.423	18.059		18.692		0.718				
		23:27:30.74	17.749	18.879	18.833	18.864	18.824	0.148	0.147	0.217	1.194	16.3
		23:29:14.77	17.731	18.862		18.847		0.147				
		23:30:58.85	17.677	18.808		18.802		0.147				
		23:32:42.80	17.651	18.783		18.783		0.146				
	2016/11/30	01:15:14.08	17.900	19.241	19.263	19.654	19.632	0.387	0.388	0.199	1.165	23.9
		01:16:38.14	17.919	19.260		19.607		0.388				
		01:18:02.06	17.949	19.289		19.636		0.388				
2005 TF	2016/10/03	03:18:42.55	19.969	20.625	20.649	20.647	20.656	0.422	0.421	0.253	1.245	13.5
		03:22:48.85	19.968	20.624		20.628		0.422				
		03:26:54.33	20.040	20.697		20.693		0.421				
	2016/10/05	03:33:16.33	19.904	20.577	20.540	20.528	20.557	0.621	0.625	0.242	1.235	12.5
		03:37:21.17	19.883	20.557		20.518		0.622				
		03:57:56.44	19.804	20.484		20.570		0.627				
		04:02:00.63	19.860	20.541		20.610		0.629				
	2016/10/24	04:11:21.35	18.508	19.896	19.858	19.896	19.832	0.151	0.154	0.153	1.148	4.4
		04:15:25.91	18.492	19.879		19.864		0.152				
		04:19:30.67	18.458	19.843		19.816		0.154				
		04:23:34.91	18.464	19.848		19.805		0.155				
		04:27:39.14	18.442	19.824		19.774		0.157				
	2016/10/27	03:34:20.70	18.371	19.868	19.874	19.924	19.898	0.231	0.232	0.143	1.136	4.6
		03:36:24.55	18.374	19.870		19.906		0.232				
		03:38:29.11	18.377	19.871		19.881		0.232				
		03:40:33.35	18.390	19.884		19.881		0.233				
	2016/10/28	02:46:12.25	18.436	20.053	20.082	20.050	0.237	0.246	0.140	1.133	4.8	
		02:48:16.00	18.452	20.069		20.066		0.237				
		02:50:19.89	18.486	20.103		20.103		0.237				
		02:52:23.91	18.485	20.102		20.105		0.271				
(36236) 1999 VV	2016/11/26	04:26:59.35	19.227	16.309	16.233	16.233	16.212	0.021	0.020	0.896	1.868	7.6
		04:30:03.93	19.120	16.202		16.202		0.019				
		04:33:08.02	19.161	16.243		16.241		0.021				
		04:36:12.15	19.096	16.178		16.173		0.020				
	2016/11/30	05:12:42.81	19.297	16.254	16.244	16.254	16.243	0.447	0.451	0.908	1.873	8.8
		05:14:47.72	19.292	16.245		16.245		0.451				
		05:16:52.05	19.284	16.232		16.230		0.455				
	2016/12/03	04:56:33.28	19.362	16.318	16.283	16.366	16.356	0.293	0.327	0.921	1.877	10.4
		05:21:31.01	19.358	16.275		16.356		0.332				
		05:24:57.31	19.338	16.248		16.330		0.339				
		05:28:21.67	19.387	16.291		16.373		0.345				
	2016/12/04	04:29:51.13	19.471	16.432	16.405	16.408	16.390	0.294	0.311	0.926	1.878	11.1
		04:33:34.83	19.442	16.399		16.375		0.298				
		04:40:28.28	19.437	16.385		16.368		0.307				

Table A4 – *continued*

Asteroid	Date	UT	M_{obs}	M_{red}	$\overline{M_{red}}$	M_{cor}	$\overline{M_{cor}}$	ΔM	$\overline{\Delta M}$	Δ (au)	r (au)	α (°)
		04:47:55.85	19.473	16.412		16.401		0.316				
		04:51:41.35	19.464	16.397		16.389		0.322				
		04:56:59.44	19.481	16.406		16.401		0.330				
	2016/12/05	04:28:17.67	19.524	16.499	16.520	16.503	16.536	0.095	0.097	0.932	1.879	11.7
		04:32:21.66	19.544	16.521		16.534		0.097				
		04:36:25.66	19.526	16.504		16.524		0.098				
		04:40:29.89	19.576	16.556		16.583		0.100				
	2016/12/07	03:38:05.22	19.708	16.621	16.571	16.619	16.575	0.325	0.331	0.944	1.882	13.0
		03:42:10.06	19.735	16.644		16.645		0.329				
		03:46:14.11	19.624	16.529		16.534		0.333				
		03:50:18.47	19.589	16.490		16.504		0.337				
(138846) 2000 VJ61	2016/11/26	04:57:10.30	19.727	16.832	16.914	16.832	17.081	0.025	0.028	0.927	1.787	21.7
		05:00:14.35	19.661	16.766		16.964		0.031				
		05:03:18.33	19.887	16.992		17.205		0.026				
		05:09:38.90	19.962	17.067		17.324		0.032				
	2016/11/29	05:54:51.44	19.509	16.832	16.803	16.943	16.912	0.169	0.169	0.884	1.764	20.5
		05:57:55.24	19.464	16.787		16.897		0.169				
		06:00:59.13	19.487	16.809		16.917		0.169				
		06:04:02.95	19.462	16.783		16.890		0.170				
	2016/12/03	06:34:25.02	19.232	16.612	16.614	16.780	16.737	0.269	0.261	0.829	1.734	18.8
		06:37:28.95	19.232	16.635		16.788		0.246				
		06:40:33.47	19.228	16.606		16.714		0.271				
		06:43:37.60	19.229	16.603		16.712		0.247				
		06:49:55.00	19.240	16.616		16.693		0.273				
	2016/12/05	04:54:44.53	19.115	16.597	16.600	16.708	16.708	0.084	0.084	0.803	1.718	17.9
		04:58:08.95	19.106	16.588		16.697		0.084				
		05:01:50.28	19.129	16.611		16.720		0.084				
2016 WJ1	2016/1127	03:57:05.69	19.627	21.533	21.549	21.453	21.498	0.162	0.164	0.164	1.150	5.5
		04:00:09.49	19.623	21.528		21.480		0.163				
		04:03:13.14	19.688	21.592		21.552		0.164				
		04:06:16.92	19.643	21.545		21.507		0.166				
	2016/11/29	04:28:46.67	19.420	21.567	21.592	21.548	21.579	0.187	0.190	0.148	1.133	7.7
		04:31:51.72	19.467	21.612		21.597		0.189				
		04:34:56.13	19.450	21.593		21.581		0.191				
		04:38:00.41	19.455	21.596		21.591		0.194				
	2016/12/02	02:22:05.86	19.172	21.799	21.821	21.801	21.820	0.226	0.226	0.119	1.100	15.3
		02:24:39.91	19.190	21.816		21.816		0.226				
		02:27:14.08	19.222	21.848		21.842		0.227				
	2016/12/04	03:29:18.10	19.100	21.851	21.844	21.763	21.761	0.290	0.294	0.111	1.091	18.0
		03:32:22.28	19.076	21.824		21.738		0.293				
		03:35:26.28	19.090	21.835		21.752		0.296				
		03:38:30.56	19.123	21.865		21.790		0.299				
	2016/12/05	03:46:35.63	19.025	21.968	22.029	21.968	21.999	0.102	0.104	0.104	1.082	20.9
		03:49:59.66	19.092	22.036		22.030		0.104				
		03:53:24.05	19.084	22.030		22.020		0.105				
		03:56:48.10	19.138	22.085		21.980		0.107				
	2016/12/07	02:45:05.38	19.051	22.255	22.347	22.166	22.241	0.350	0.358	0.091	1.065	27.5
		02:51:23.10	18.938	22.135		22.022		0.357				
		02:54:47.27	19.325	22.518		22.405		0.361				
		02:58:11.50	19.292	22.480		22.370		0.366				

This paper has been typeset from a TEX/LATEX file prepared by the author.